The American Journal of Pathology, Vol. 172, No. 3, March 2008

DOI: 10.2353/ajpath.2008.070312

Vascular Biology, Atherosclerosis and Endothelium Biology

Potential Role of CYLD (Cylindromatosis) as a Deubiquitinating Enzyme in Vascular Cells

Yoichi Takami,*† Hironori Nakagami,† Ryuichi Morishita,‡ Tomohiro Katsuya,* Hiroki Hayashi,† Masaki Mori,† Hiroshi Koriyama,* Yoshichika Baba,* Osamu Yasuda,* Hiromi Rakugi,* Toshio Ogihara,* and Yasufumi Kaneda†

From the Department of Geriatric Medicine, and the Divisions of Gene Therapy Science,† and Clinical Gene Therapy,‡ Osaka University Graduate School of Medicine, Osaka, Japan*

Data from several studies suggest that the ubiquitin-proteasome system may play a role in the progression of atherosclerosis. Here, we examined the potential role of the deubiquitinating enzyme CYLD (cylindromatosis), mutation of which has been reported to cause familial cylindromatosis. Northern blot analysis revealed expression of CYLD mRNA in the aorta, as well as in cultured human aortic endothelial cells (ECs) and vascular smooth muscle cells. Treatment with recombinant tumor necrosis factor (TNF)-α significantly increased CYLD expression in ECs and vascular smooth muscle cells. Immunostaining showed CYLD expression in atherosclerotic lesions from human carotid arteries and up-regulation of CYLD expression in the neointima of rat carotid arteries after balloon injury. Overexpression of CYLD in ECs resulted in inhibition of TNF-α-induced nuclear factor-κB activity through deubiquitination of TNFR-associated factor 2 (TRAF2), whereas overexpression of catalytically inactive CYLD had no effect. CYLD overexpression also inhibited expression of cyclin D1 and activation of the E2F pathway through deubiquitination of the upstream molecule Bcl-3 and inhibition of its translocation into the nucleus. Overexpressed CYLD also significantly inhibited cell viability. Furthermore, overexpression of CYLD in rat balloon-injured carotid artery attenuated neointimal formation through inactivation of nuclear factor-κB and E2F. In conclusion, these data demonstrate that the deubiquitinating enzyme CYLD may inhibit inflammation and proliferation in vascular cells and may represent a novel target for the treatment or prevention of atherosclerosis. ***(Am J Pathol 2008, 172:818–829; DOI: 10.2353/ajpath.2008.070312)***

Ubiquitination regulates a wide variety of cellular processes, including degradation of proteins, receptor endocytosis, DNA repair, gene transcription, the cell cycle, inflammation, and immune response.[1] Protein ubiquitination is a reversible process, and ubiquitin can be cleaved from its protein substrates by deubiquitinating enzymes (DUBs). Thus, similar to protein phosphorylation, regulated ubiquitination and deubiquitination of specific substrates are instrumental in cellular signaling.[1]

The vasculature is capable of sensing changes within its milieu, integrating these signals by intercellular communication, and changing itself through the local production of mediators that influence structure as well as function (eg, vascular remodeling).[2] DUBs reverse the ubiquitination process via disassembly of the polyubiquitin chain, recycling active ubiquitin by the removal of ubiquitin from its covalently linked protein, and generating monomeric ubiquitin from its precursor fusion protein.[3] Although the proteasome inhibitor, MG132, inhibits degradation of ubiquitinated proteins and can reduce neointimal formation,[4] it has not been clarified whether or how DUBs are involved in vascular remodeling.

Mutations of the tumor suppressor gene, *CYLD*, result in familial cylindromatosis, also called "turban tumor syndrome," an autosomal-dominant condition that predisposes to multiple skin tumors.[5] The product of *CYLD* is a DUB recently implicated in suppression of the nuclear factor (NF)-κB pathway, a crucial mediator of immune responses, inflammation, and vascular remodeling.[3] Activation of NF-κB plays a pivotal role in the coordinated transactivation of cytokine and adhesion molecule genes involved in atherosclerosis, and blockade of NF-κB significantly attenuated neointimal formation of vascular smooth muscle cells (VSMCs).[6] Although CYLD expression has been characterized in multiple tissue types, its

Supported by the Northern Osaka (Saito) Biomedical Knowledge-Based Cluster Creation Project, the Mitsubishi Pharma Research Foundation (to Y.K.), the Salt Science Research Foundation (to T.O.), the Takeda Science Foundation (to T.O.), and the Japan Heart Foundation (to T.K. and H.N.).

Accepted for publication November 20, 2007.

Address reprint requests to Hironori Nakagami, M.D., Ph.D., Department of Gene Therapy Science, Osaka University Graduate School of Medicine, 2-2 Yamada-oka, Suita 565-0871, Japan. E-mail: nakagami@gts.med.osaka-u.ac.jp.

role in the vasculature remains unknown. Because we identified the expression of CYLD in both vascular endothelial cells (ECs) and smooth muscle cells in this study, and the attenuation of NF-κB signaling by CYLD was expected to bring about anti-inflammatory and anti-proliferative activity leading to anti-atherosclerotic and anti-vascular remodeling actions, we examined the function of CYLD, especially focusing on NF-κB activity in the vasculature.

Materials and Methods

Cell Culture and MTS Assay

Human aortic endothelial cells (HAECs), human aortic smooth muscle cells (HASMCs), and bovine aortic endothelial cells (BAECs) were purchased from Clonetics Corp. (Palo Alto, CA). A7r5 (embryonic thoracic aorta, smooth muscle, DB1X rat) and THP-1 cells were obtained from the American Type Culture Collection (Rockville, MD) and were maintained as previously described.[7] Cell viability was measured using the MTS [3-(4,5-dimethylthiazol-2-yl)-5-(3-carboxymethoxyphenyl)-2-(4-sulfophenyl)-2H-tetrazolium] assay. Ten μl of CellTiter 96 One Solution reagent (Promega, Madison, WI) was added to each well, and absorbance at 490 nm was measured.

Materials and Plasmid DNA Construction

Recombinant tumor necrosis factor (TNF)-α was obtained from PeproTec (London, UK). Other materials were obtained from Sigma Chemical Co. (St. Louis, MO). A hypoxic condition was prepared using a BBL GasPak (Becton Dickinson, Franklin Lakes, NJ), which catalytically reduces oxygen to undetectable levels within 90 minutes as previously described.[8]All of the cell transfection in this study was performed using Lipofectamine 2000 (Invitrogen, Carlsbad, CA) in accordance with the manufacturer's instructions. Gateway cloning technology (Invitrogen) was used to construct expression vectors in accordance with the manufacturer's instructions. Briefly, human CYLD was subcloned into D-TOPO to construct entry vectors. Two different types of catalytically inactive mutants of CYLD were constructed by deletion of the catalytic domain (CYLDdel), which corresponds to ubiquitin carboxyl-terminal hydrolase type 2-1 (UCH2-1, amino acids 593 to 610)[5] and amino acid replacement in this catalytic domain (C601A, $CYLD_{C/A}$).[9]These entry vectors were then transferred into the mammalian expression vectors, pcDNA3.1 and pCAGGS,[10] through an LR-recombination reaction, creating pcDNA3.1-CYLD, pcDNA3.1-CYLDdel, pcDNA3.1-$CYLD_{C/A}$, pCAGGS-FLAG-CYLD, and pCAGGS-FLAG-$CYLD_{C/A}$. HA-tagged ubiquitin expression vector (HA-Ub) was constructed by subcloning into pcDNA3 vector. pcDNA3.1-GFP, -luciferase, or -lacZ was used as a control vector. Overexpression of these control vectors showed no significant difference in several assays performed in this study compared with pcDNA3.1 empty vector.

Northern Blotting and Real-Time Reverse Transcriptase-Polymerase Chain Reaction (RT-PCR)

Northern blotting was performed as previously described.[11] Total RNA of cells or tissue samples was extracted using an RNeasy mini kit (Qiagen, Valencia, CA) or Isogen (Nippon Gene, Toyama, Japan). Equal aliquots of total RNA (5 μg) were separated by 1% formaldehyde-agarose gel electrophoresis, and hybridization and washing were performed. Part of human CYLD cDNA was used as a probe. Loading conditions were determined by reprobing with GAPDH or 18S ribosomal RNA. Human 12-lane MTN blot (no. 7780-1; Clontech Laboratories, Inc., Mountain View, CA) and human cardiovascular system MTN blot (no. 7791-1; Clontech Laboratories, Inc.) were prepared from high-quality poly(A)$^+$ RNA and normalized against the GAPDH hybridization signal (Clontech) according to the manufacturer's instructions.

Complementary DNA was synthesized using the Thermo Script RT-PCR system (Invitrogen). Relative gene copy numbers were quantified by real-time RT-PCR using TaqMan gene expression assays (human CYLD,: Hs 00211000; rat interleukin (IL)-6, Rn00561420; rat matrix metalloproteinase (MMP)-9, Rn00579162; and 18S ribosomal RNA, Hs99999901; Applied Biosystems, Foster City, CA) or Cyber Green gene expression assays using SYBR Premix Ex Taq (Takara Bio, Inc., Madison, WI). The absolute number of gene copies was normalized using 18S ribosomal RNA or GAPDH and standardized to a sample standard curve. Specific primers for Cyber Green Gene expression assay were: bovine GAPDH forward: 5′-GAGGGACTTATGACCACTGTCCAC-3′, reverse: 5′-GGGCCATCCACAGTCTTCTG-3′; bovine ICAM-1 forward: 5′-TCACCGTATACTGGTTCCCGGAG-3′, reverse: 5′-GAGTTCTTCACCCACAGGCTGC-3′; bovine VCAM-1 forward: 5′-AATTAACTGTTCAAGAGAAAAACTTTACTGTT-3′, reverse: 5′-CACGACTGAGTCGCCAACC-3′; bovine E-selectin forward: 5′-CTACTGCTGGAGTCTCCCTTGTGAC-3′, reverse: 5′-GGCTTGAGCAGCTGCTGGCAGGAGA-3′; rat CYLD forward: 5′-GCAGTGTAACAGACAAACAGACACA-3′, reverse: 5′-TTGCCTTTAGCAGAAGGAACTC-3′.

Western Blotting and Immunoprecipitation

Briefly, cell extracts were prepared with lysis buffer (RIPA buffer: 150 mmol/L NaCl, 1% Nonidet P-40, 0.5% deoxycholate-Na, 0.1% sodium dodecyl sulfate, 50 mmol/L Tris-HCl, pH 8.0, and ethylenediaminetetraacetic acid-free protease inhibitor cocktail; Roche Applied Science, Mannheim, Germany). Samples containing 5 μg of protein were separated on 10% sodium dodecyl sulfate-polyacrylamide electrophoresis gels and transferred to nitrocellulose membranes (Hybond ECL; GE Health Care, Arlington Heights, IL), and incubated with anti-cyclin D1 monoclonal antibody (1:2000; Cell Signaling Technology, Beverly, MA), anti-Bcl-3 antibody (1:200, sc-185; Santa Cruz Biotechnology Inc., Santa Cruz, CA), and anti-β-actin (1:5000, Sigma) at 4°C overnight. The

membranes were then washed and incubated with a 1:2000 dilution of mouse or rabbit IgG horseradish peroxidase-conjugated antibody (GE Health Care). Bound antibodies were detected by enhanced chemiluminescence (ECL, GE Health Care) with Hyperfilm-MP (GE Health Care).

For immunoprecipitation, lysates were obtained from BAECs that were transfected using Lipofectamine 2000 with control vector, pcDNA3.1-CYLD plasmid, or pcDNA3.1-$CYLD_{C/A}$ plasmid together with HA-Ub. The cells were stimulated with TNF-α (10 ng/ml) for 5 minutes and the lysates were precleared for 60 minutes at 4°C. After immunoprecipitation with anti-TRAF2 antibody (1.0 μg per 100 μg of protein in lysis buffer; Santa Cruz Biotechnology, Inc.), ubiquitinated TRAF2 was evaluated by immunoblotting with anti-HA antibody (1:3000, Sigma) to detect HA-ubiquitin. To test the protein input, a small part of the resulting lysates was also immunoblotted using anti-TRAF2 and anti-β-actin antibodies.

In Vivo *Gene Transfer into Rat Balloon-Injured Carotid Artery*

Rat balloon-injured carotid arteries were prepared from wild-type male Sprague-Dawley rats (weight, 400 to 500 g; Charles River Breeding Laboratories, Wilmington, MA) as described previously.[12] The HVJ-liposome method was used for transfection of plasmid DNA into rat carotid artery. HVJ-AVE liposomes were prepared as described previously.[13] Briefly, plasmid DNA diluted in balanced salt solution and a dried AVE lipid mixture were shaken vigorously, and then sonicated to form unilamellar liposomes. Purified HVJ was inactivated by UV radiation and then added. The HVJ-liposome mixture was kept on ice for 10 minutes, and then incubated at 37°C with shaking for 1 hour to form fusigenic HVJ-AVE liposomes. After 30% sucrose density gradient ultracentrifugation, the HVJ-AVE liposomes were visualized in a layer between balanced salt solution and 30% sucrose solution, whereas free HVJ sediment was at the bottom. The HVJ-AVE liposomes were collected and suspended in balanced salt solution to obtain HVJ-AVE liposome-plasmid complex.

A cannula was introduced into the common carotid artery through the external carotid artery. Then the HVJ-liposome complex was infused into the segment and incubated for 10 minutes at room temperature. After a 10-minute incubation, the infusion cannula was removed. After transfection, blood flow to the common carotid artery was restored by release of the ligatures, and the wound was closed. Each carotid artery was processed for immunochemical staining at 7 days after injury and transfection, and for morphological study at 2 weeks after injury. Cross sections of carotid artery were stained with hematoxylin and eosin (H&E) and photographed. The intimal and medial cross-sectional areas of the carotid arteries were measured using Image J (National Institutes of Health, Bethesda, MD), and the intima/media ratios of cross sections were calculated. At least three individual sections from the middle of the transfected arterial segments were analyzed.

Immunohistochemical Staining

Cells on glass coverslips were fixed in 4% paraformaldehyde for 15 minutes and then permeabilized with 0.2% Triton X-100 for 5 minutes. After blocking in 5% skimmed milk, samples were incubated with anti-CYLD antibody (1:50, sc-25779; Santa Cruz Biotechnology, Inc.), anti-p65 antibody (1:100, sc-372; Santa Cruz Biotechnology Inc.), anti-Bcl-3 antibody (1:100, sc-185; Santa Cruz Biotechnology, Inc.), or monoclonal anti-FLAG M2 antibody (1:500, Sigma) at 4°C overnight. Corresponding secondary antibodies were labeled with Alexa Fluor 488 or 546 (1:200; Molecular Probes, Eugene, OR).

Sections of intact or balloon-injured rat carotid arteries were fixed in 4% paraformaldehyde or cold methanol for 15 minutes and then immunostained as aforementioned. Primary antibodies used for immunofluorescent staining were anti-CYLD antibody (1:50, sc-25779; Santa Cruz Biotechnology, Inc.), anti-p65 (1:100; Chemicon International, Inc., Temecula, CA), anti-ICAM-1 (1:100, sc-1511; Santa Cruz Biotechnology, Inc.), and anti-PCNA (1:1000, clone PC10; DAKO, Carpinteria, CA) antibodies. Anti-p65 antibody used for immunohistological studies recognizes epitopes overlapping the nuclear location signal of the subunit of the NF-κB heterodimer. Thus, this antibody selectively binds to the activated form of NF-κB. To rule out nonspecific staining in each immunofluorescence experiment, a negative control was performed with nonimmunized IgG matching the host species and concentration of the primary antibody, and all negative controls in this study were not stained in the observed area of interest (data not shown). As for the quantification of ICAM-1- and PCNA-positive cells in the neointima at 7 days after balloon injury, a total of 10 different fields from each balloon-injured artery were randomly selected, and the percentage of immunopositive cells against the total number of nuclei (4,6-diamidino-2-phenylindole, DAPI) was calculated. All experimental protocols were approved by the Osaka University Graduate School of Medicine Standing Committee on Animals.

Human tissue specimens were obtained from patients who underwent carotid end-atherectomy for symptomatic high-grade carotid stenosis. After surgery, plaques were fixed in formalin and embedded in paraffin for histological examination. Sections were serially cut at 5 μm, and mounted on lysine-coated slides. For immunostaining with anti-CYLD antibody (1:50, sc-25779; Santa Cruz Biotechnology, Inc.), we used an avidin-biotin horseradish peroxidase visualization system (Vectastain ABC kit and DAB substrate kit for peroxidase; Vector Laboratories, Burlingame, CA). For immunofluorescent staining, we treated the samples with antigen retrieval reagents using HistoVT One (Nacalai Tesque, Kyoto, Japan), and stained them with anti-α-smooth muscle actin antibody (1:200, Sigma) and anti-Alexa Fluor 488 (1:200, Molecular Probes) as corresponding secondary antibodies. Informed consent was obtained from all patients, and the

protocols were also approved by the Ethics Committee of Osaka University.

Evaluation by Reporter Gene and Gel Mobility Shift Assay

Genes were transfected into BAECs or A7r5 along with a luciferase gene driven by the NF-κB binding site (NF-κB-luciferase reporter gene; BD Bioscience Clontech, Palo Alto, CA) or by the E2F binding site (E2F-luciferase reporter gene, BD Bioscience Clontech) and PRL-TK plasmids (Promega) using Lipofectamine 2000 (Invitrogen, Grand Island, NY). After transfection, luciferase activity was measured with the dual-luciferase assay system (Promega) after incubation with serum-free Dulbecco's modified Eagle's medium for 24 hours. PRL-TK plasmids (Renilla-luciferase-expression plasmids) were used for normalizing cell viability or transfection efficiency.

Nuclear extract was prepared from cultured A7r5 or from BAECs overexpressing a control gene or human CYLD using NE-PER (Promega), according to the manufacturer's instructions. Gel mobility shift assay was performed using a gel shift assay system (Promega) according to the manufacturer's instructions. Briefly, NF-κB consensus oligodeoxynucleotides (5′-AGTTGAG*GGGA-CTTTCC*AGGC-3′) or E2F-consensus oligodeoxynucleotides (5′-ATTTAAGT*TTCGCGCC*CTTTCTCAA-3′) were labeled with ^{32}P and purified using a Nick column (Pharmacia Biotech, Inc., Piscataway, NJ) (consensus sequences are italicized). Binding reactions (10 μl), including ^{32}P-labeled probe (0.5 to 1 ng; 10,000 to 15,000 cpm), were incubated with 5 μg of nuclear extract in 1 mmol/L $MgCl_2$, 50 mmol/L NaCl, 50 mmol/L Tris-HCl, pH 7.5, 0.5 mmol/L ethylenediaminetetraacetic acid, 0.5 mmol/L dithiothreitol, 4% glycerol, and 0.05 mg/ml poly(deoxyinosinic-deoxycytidylic) acid in a total of 10 μl for 30 minutes at room temperature and then loaded onto a 4% polyacrylamide gel. Specificity of binding was ascertained by competition with a 160-fold molar excess of unlabeled consensus oligonucle-

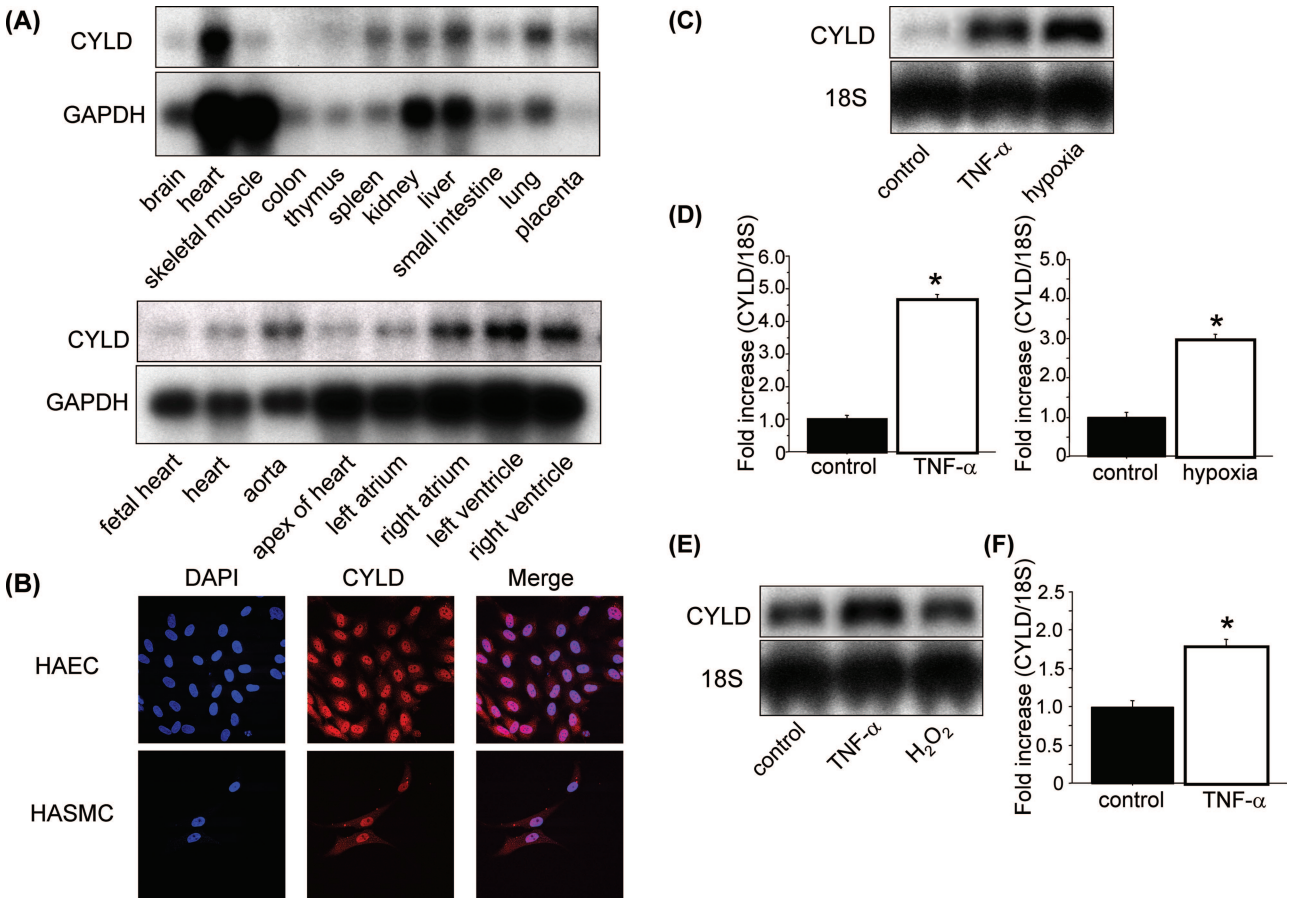

Figure 1. Expressional analysis of CYLD. **A:** Representative Northern blot of human CYLD in several human tissues and cardiovascular tissues. **Top:** CYLD is ubiquitously expressed in several tissues and is expressed in the human heart. **Bottom:** Human CYLD is expressed in the aorta as well as the heart. Corresponding GAPDH expression was used to standardize loading. **B:** Immunofluorescent staining with anti-CYLD antibody (CYLD, red) and nuclear staining (DAPI, blue) in HAECs (**top**) and HASMCs (**bottom**). Human CYLD expression was localized in the nucleus and cytoplasm in both cells. **C** and **D:** Northern blot (**C**) and quantitative real time PCR (**D**) of human CYLD in HAECs. After treatment with recombinant TNF-α (10 ng/ml) or a hypoxic condition for 24 hours, expression of human CYLD was markedly increased. Corresponding 18S ribosomal RNA expression was used to standardize loading. Experiments were performed in duplicate for Northern blot. $^*P < 0.05$ versus control. $N = 4$ for quantitative real-time PCR. **E** and **F:** Northern blot (**E**) and quantitative real-time PCR (**F**) of human CYLD in HASMCs. After treatment with recombinant TNF-α (10 ng/ml) for 24 hours, expression of human CYLD was markedly increased, but was not significantly altered after treatment with hydrogen peroxide (H_2O_2, 100 μmol/L) for 24 hours. Corresponding 18S ribosomal RNA expression was used to standardize loading. Experiments were performed in duplicate for Northern blot. $^*P < 0.05$ versus control. $N = 4$ for quantitative real-time PCR. Original magnifications, ×600.

otides. The gels were subjected to electrophoresis, drying, and autoradiography.

Adhesion Assay

Adhesion of the THP-1 human monocyte cell line to BAECs was assessed as previously described.[14] THP-1 cells were labeled with fluorescein isothiocyanate using a PKH67 fluorescent staining kit (Zynaxis, Inc., Malvern, PA) according to the manufacturer's instructions. Fluorescein isothiocyanate-labeled THP-1 cells (5×10^5 cells/well) were incubated with BAECs in 24-well plates for 10 minutes at 37°C, and then each well was washed with phosphate-buffered saline three times to separate nonadherent monocytes. Adherent cells were lysed with 50 mmol/L Tris (pH 8.4)/0.1% sodium dodecyl sulfate, and the fluorescence was measured.

Statistical Analysis

All values are expressed as mean ± SE. Analysis of variance with subsequent Fisher's PLSD test or unpaired Student's *t*-test was used to determine the significance of differences in multiple comparisons. All statistical analysis was performed using Stat-View 5.0 software (SAS Institute, Inc., Cary, NC).

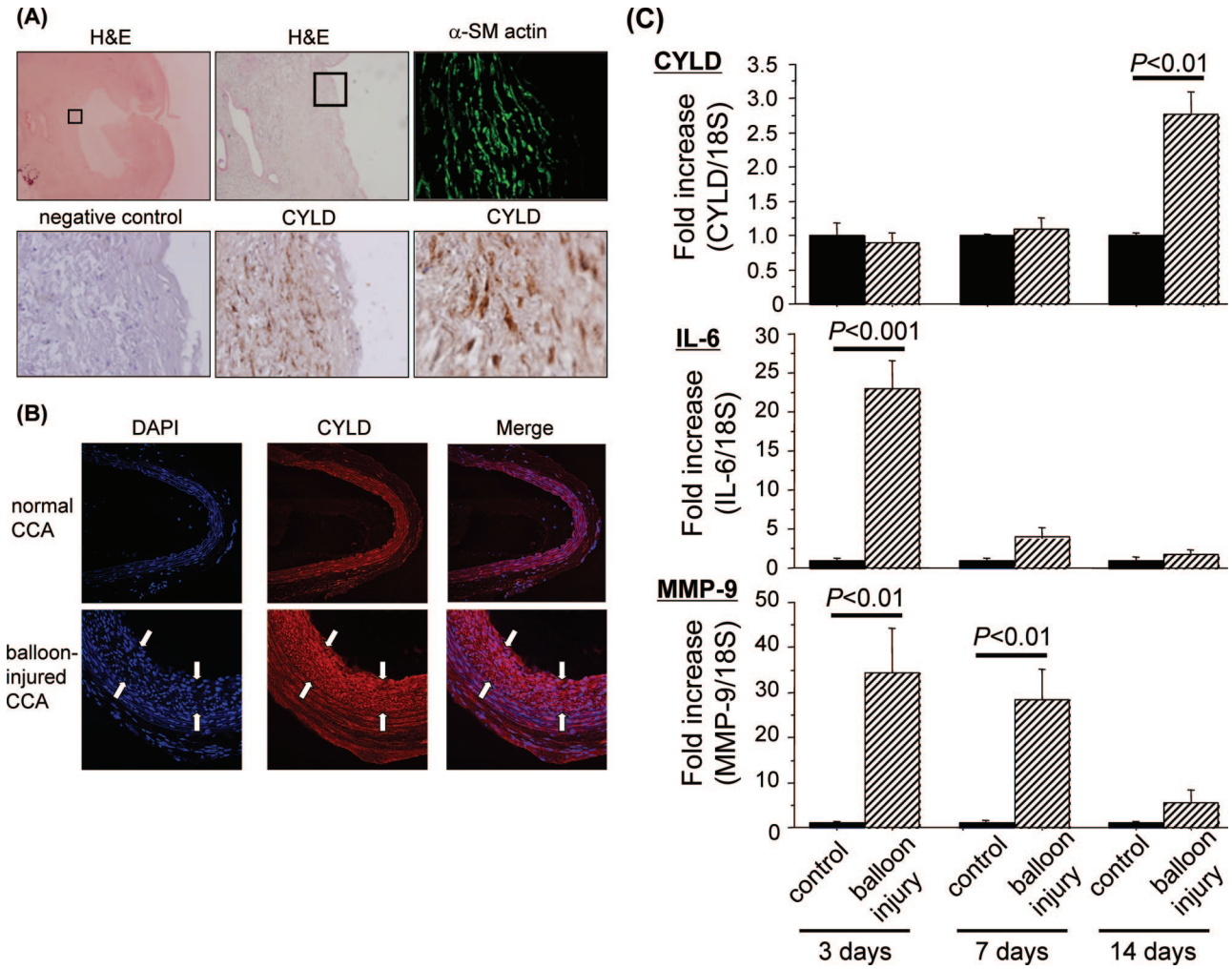

Figure 2. Expressional analysis of CYLD in human carotid atherosclerotic lesions and rat common carotid artery after balloon injury. **A:** Representative photomicrographs of immunochemical staining with anti-CYLD antibody in human carotid atherosclerotic lesions. We examined the specimens obtained from four patients (68-year-old man, 74-year-old man, 72-year-old man, and 64-year-old woman) who underwent carotid end-atherectomy for symptomatic high-grade carotid stenosis (78 to 88% stenosis). All of them had multiple lacunar infarction on computed tomography and some risk factors (eg, hypertension, hyperlipidemia, and diabetes). We have shown one sample from among them—a piece of atherosclerotic lesion of the left carotid artery (88% stenosis) obtained from a 74-year-old man with hypertension. H&E staining shows the corresponding atherosclerotic lesion of human carotid artery. The **squares** in **left top** and **middle top** panel show the examined area for histological analysis. Immunochemical staining with a smooth muscle-specific marker, anti-smooth muscle actin (α-SM actin, green), and anti-CYLD antibody (CYLD; brown) and nuclear staining (hematoxylin, blue) of the human carotid atherosclerotic lesion were performed. Negative control indicates nonimmunized IgG matching the host species and concentration of anti-CYLD antibody. These sections are serial. **B:** Immunofluorescent staining with anti-CYLD (CYLD, red) in rat carotid artery. **Top:** CYLD was expressed in the normal rat carotid artery. **Bottom:** Immunofluorescent staining with anti-CYLD antibody (CYLD, red) and nuclear staining (DAPI, blue) in rat balloon-injured carotid artery. The area between the **white arrows** is neointimal formation. Expression of CYLD was up-regulated in the neointima of balloon-injured artery. **C:** Quantification of CYLD, IL-6, and MMP-9 expression in rat common carotid arteries by quantitative real-time RT-PCR at 3, 7, and 14 days after balloon injury. Results are expressed as the ratio of relative gene expression of CYLD in balloon-injured carotid artery (balloon injury) compared to that in the carotid artery on the opposite side to the balloon-injury procedure (control). $N = 5$ per group in duplicate. Original magnifications: ×10 (**A**, **top left**); ×40 (**A**, **top middle**); ×200 [**A** (**top right**, **middle bottom**, **bottom left**), **B**]; ×600 (**A**, **bottom right**).

Results

Expression of CYLD in the Cardiovascular System

Northern blot analysis demonstrated that human CYLD mRNA was ubiquitously expressed in several tissues, and was expressed in the heart as shown in the top panel of Figure 1A. The expression level of human CYLD mRNA in the aorta was similar to that in the heart, as shown in the bottom panel of Figure 1A. Immunofluorescent staining showed that CYLD protein was expressed in HAECs and HASMCs, and was located in both the nucleus and cytoplasm (Figure 1B). We confirmed that CYLD protein was not stained with nonimmunized IgG matching the host species and concentration of the primary antibody,

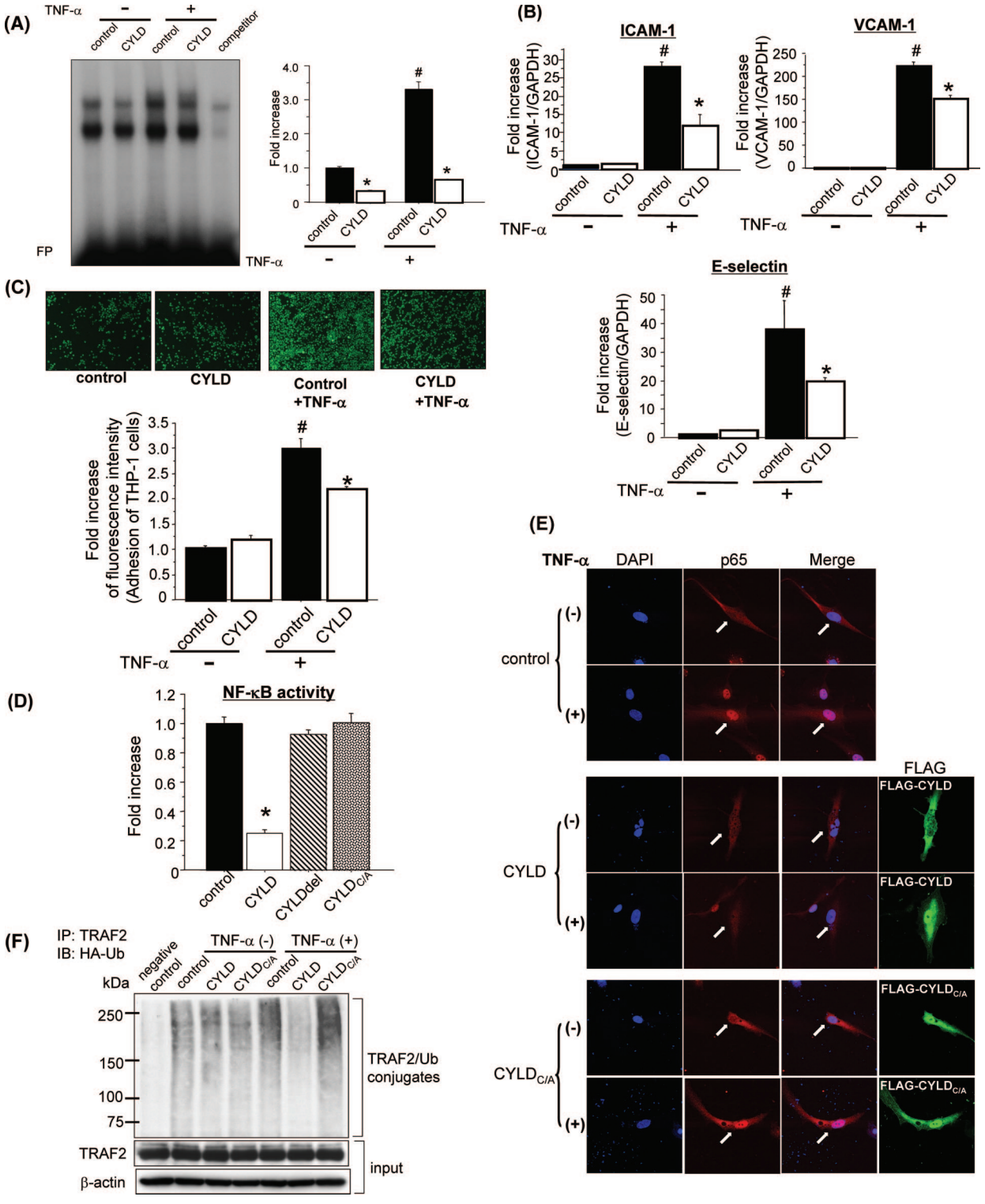

to establish the specificity of the anti-CYLD antibody used in this study (data not shown). In HAECs, CYLD mRNA level was significantly increased after a 24-hour treatment with TNF-α (10 ng/ml) or under hypoxic conditions (Figure 1C). Real-time PCR demonstrated similar results in terms of CYLD expression in response to TNF-α (4.6-fold increase, $P < 0.05$ versus control) and under hypoxic conditions (3.0-fold increase, $P < 0.05$ versus control) (Figure 1D). Treatment with TNF-α increased the CYLD mRNA level in HASMCs as assessed by Northern blot and real-time PCR (1.8-fold increase, $P < 0.05$ versus control), whereas hydrogen peroxide (H_2O_2, 100 μmol/L) did not increase CYLD mRNA (Figure 1, E and F).

Immunostaining Analysis of CYLD Expression

We examined CYLD expression in atherosclerotic lesions from human carotid arteries. H&E staining showed the corresponding atherosclerotic plaque in the sample. Immunofluorescent staining showed high expression of CYLD protein in VSMCs, as verified by co-staining with anti-α-smooth muscle actin antibody (Figure 2A). We examined CYLD expression in a balloon-injury model of the rat common carotid artery. Immunostaining analysis demonstrated that CYLD was endogenously expressed in rat carotid artery, and was up-regulated in the neointima of rat balloon-injured carotid artery at 14 days after injury (Figure 2B). We quantified the time course change of CYLD mRNA expression in rat balloon-injured common carotid artery. The expression of CYLD mRNA was significantly up-regulated at 14 days after injury (2.8-fold increase, $P < 0.01$ versus control), but not at 3 days and 7 days, whereas the expression of IL-6 and MMP-9 were highly up-regulated at 3 days, to a lesser extent at 7 days, but not at 14 days after injury (Figure 2C). These results suggest that induction of CYLD expression in the injured artery was delayed after the up-regulation of inflammatory cytokines.

Functional Analysis of Effect of CYLD on NF-κB Activity in ECs

We examined the effect of CYLD on NF-κB activity in ECs. Treatment of BAECs with TNF-α (10 ng/ml) for 12 hours significantly up-regulated NF-κB activity, whereas overexpression of CYLD significantly attenuated NF-κB activity, particularly in TNF-α-stimulated samples (80% inhibition; $P < 0.01$, compared with control under TNF-α treatment) (Figure 3A). Similarly, in the gel shift mobility assay, overexpression of CYLD also inhibited binding of NF-κB to the DNA consensus sequence (Figure 3A). Overexpression of CYLD significantly attenuated TNF-α-induced expression of ICAM-1, VCAM-1, and E-selectin in BAECs (Figure 3B). Furthermore, adhesion of fluorescein isothiocyanate-labeled THP-1 cells to BAECs was also inhibited by CYLD overexpression (Figure 3C).

To examine whether the inhibitory effect of CYLD on NF-κB activity in ECs was attributable to its deubiquitinating action, we used a catalytically inactive mutant of CYLD which contained a deletion mutation of the catalytic domain (CYLDdel) or an amino acid replacement in this catalytic domain (C601A, $CYLD_{C/A}$).[9] Overexpression of CYLD significantly decreased NF-κB activity in BAECs; however, overexpression of a catalytically inactive mutant, CYLDdelor $CYLD_{C/A}$, showed no change in NF-κB activity (Figure 3D). Immunofluorescent staining with anti-p65 antibody in HAECs showed that p65, a NF-κB subunit, was rapidly translocated into the nucleus after treatment with TNF-α for 30 minutes, whereas in CYLD-transfected ECs, p65 remained predominantly in the cytoplasm after the same treatment. Of importance, catalytically inactive CYLD overexpression allowed p65 translocation into the nucleus after the same treatment (Figure 3E). Because the target of CYLD in the NF-κB pathway is known to be deubiquitination of TRAF2, we also confirmed the deubiquitination of TRAF2 by CYLD in ECs. Indeed, immunoprecipitation analysis showed that

Figure 3. Effect of CYLD on NF-κB activation in vascular aortic ECs. **A:** Overexpression of CYLD significantly attenuated NF-κB activation with or without TNF-α stimulation, as assessed by gel mobility shift assay (**top**) and by means of the luciferase gene driven by the NF-κB binding site (**bottom**) in BAECs. **Top:** Overexpressed CYLD suppressed the binding of NF-κB to the DNA consensus sequence in gel mobility shift assay. **Bottom:** Overexpressed CYLD attenuated NF-κB activity. Control indicates overexpressed GFP gene, and CYLD indicates overexpressed human CYLD. TNF-α indicates treatment with human recombinant TNF-α (10 ng/ml) for 12 hours. $^*P < 0.05$ versus control. $^{\#}P < 0.05$ versus TNF-α (−). $N = 6$ per group in triplicate. **B:** Quantitative real-time PCR of ICAM-1, VCAM-1, and E-selectin mRNA expression with or without overexpression of CYLD. Overexpressed CYLD significantly attenuated the expression of these NF-κB regulatory genes induced by treatment with TNF-α for 6 hours. Control indicates overexpressed luciferase gene, CYLD indicates overexpressed human CYLD, and TNF-α indicates treatment with human recombinant TNF-α (10 ng/ml) for 6 hours. $^*P < 0.05$ versus control under TNF-α. $^{\#}P < 0.05$ versus TNF-α (−). $N = 6$ per group in triplicate. **C:** Evaluation of adhesion of fluorescein isothiocyanate-labeled THP-1 to BAECs. **Top:** Representative pictures; **bottom:** quantification of fluorescence intensity. Overexpressed CYLD significantly attenuated TNF-α-induced attachment of monocytes to ECs. Control indicates overexpressed luciferase gene, CYLD indicates overexpressed human CYLD, and TNF-α indicates treatment with human recombinant TNF-α (10 ng/ml) for 6 hours. $^*P < 0.05$ versus control under TNF-α. $^{\#}P < 0.05$ versus TNF-α (−). $N = 6$ per group in triplicate. **D:** Effect of catalytically inactive CYLD on NF-κB activity as assessed by means of the luciferase gene driven by the NF-κB biding site in BAECs. Overexpression of CYLD significantly attenuated NF-κB activation, whereas overexpression of a catalytically inactive mutant, CYLDdelor $CYLD_{C/A}$, showed no effect. Control indicates overexpressed GFP gene, and CYLD indicates overexpressed human wild-type CYLD. CYLDdel indicates overexpressed deletion mutant of human CYLD. $CYLD_{C/A}$ indicates overexpression of mutant with amino acid replacement of human CYLD. $^*P < 0.05$ versus control. **E:** Immunostaining analysis of NF-κB subunit, p65, in HAECs with or without treatment with TNF-α (10 ng/ml) for 30 minutes. Overexpressed wild-type CYLD attenuated TNF-α-induced translocation of p65 into the nucleus, whereas overexpressed catalytically inactive CYLD did not. Control indicates immunofluorescent staining in GFP-transfected cells, CYLD indicates FLAG-tagged wild-type CYLD-transfected cells, and $CYLD_{C/A}$ indicates FLAG-tagged catalytically inactive CYLD (amino acid replacement)-transfected cells. DAPI indicates nuclear staining (blue), p65 indicates staining with anti-p65 antibody (red), and merge indicates staining with both. **Left:** Immunofluorescent staining with anti-FLAG antibody (green) in CYLD and $CYLD_{C/A}$ to confirm transfection of human CYLD, or catalytically inactive CYLD expression in HAECs. TNF-α (+) indicates treatment with TNF-α (10 ng/ml) for 30 minutes. **White arrows** indicate transfected cells. **F:** Western blot of ubiquitinated TRAF2 by immunoprecipitation in HA-Ub-transfected BAECs. Overexpressed wild-type CYLD attenuated TNF-α-induced ubiquitination of TRAF2, whereas overexpressed catalytically inactive CYLD (amino acid replacement) did not. IP:TRAF2 indicates immunoprecipitation with TRAF2 and IB:HA-Ub indicates immunoblotting with anti-HA antibody to detect HA-ubiquitin. Control indicates overexpressed GFP gene, CYLD indicates overexpressed human wild-type CYLD, and $CYLD_{C/A}$ indicates overexpressed human catalytically inactive CYLD (amino acid replacement). Negative control was immunoprecipitation with nonimmunized IgG matching the host species and amount of TRAF2 antibody. TNF-α (+) indicates treatment with TNF-α (10 ng/ml) for 5 minutes. **Middle:** Equal amounts of TRAF2 were used for immunoprecipitation. Experiments were performed in triplicate. Original magnifications, ×800.

overexpression of CYLD induced deubiquitination of TRAF2 in ECs. Of importance, overexpression of catalytically inactive CYLD did not induce deubiquitination of TRAF2 (Figure 3F). These results suggest that the inhibitory effect of CYLD on NF-κB activity is attributable to its deubiquitinating action through the deubiquitination of TRAF2.

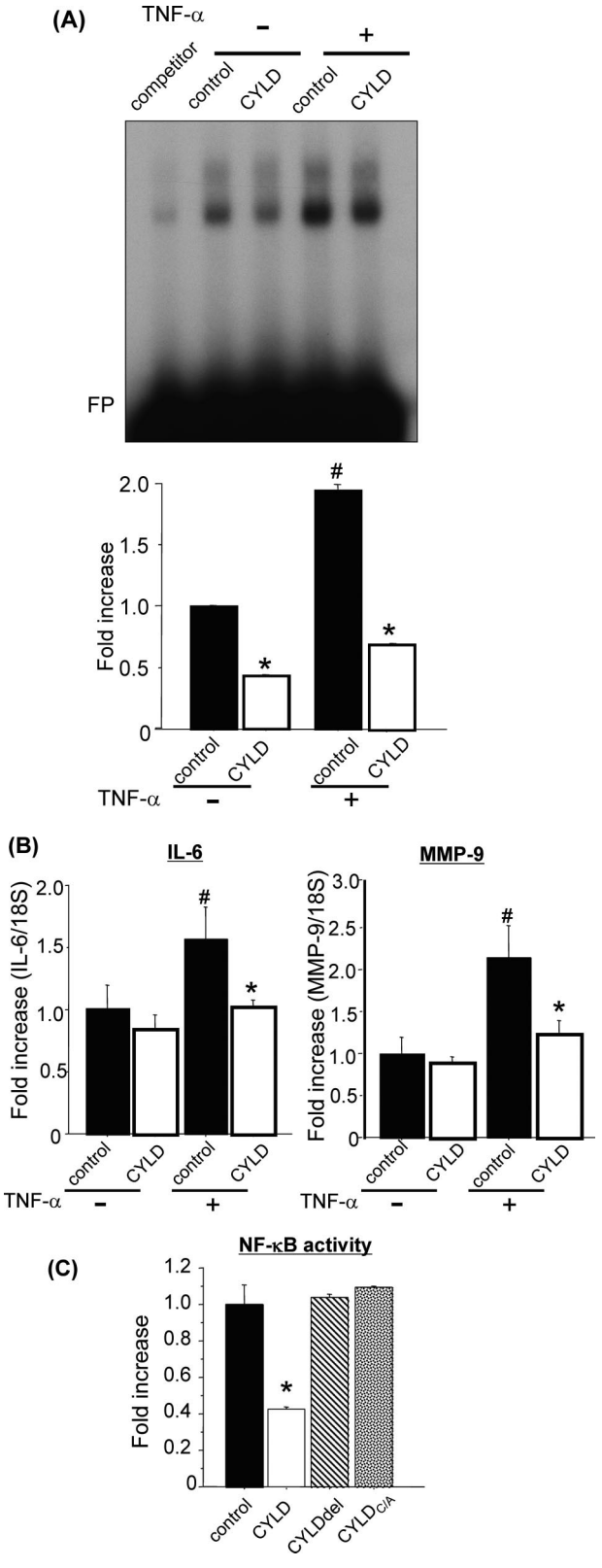

Functional Analysis of CYLD in VSMCs

In rat smooth muscle cells (A7r5), overexpression of CYLD inhibited the binding of NF-κB to the DNA consensus sequence in the gel shift mobility assay. In the reporter gene assay, overexpression of CYLD attenuated NF-κB activity, particularly in TNF-α-stimulated samples (65% inhibition; $P < 0.001$, compared with control under TNF-α treatment) (Figure 4A). In addition, overexpression of CYLD significantly suppressed NF-κB-driven gene expression (eg, IL-6 and MMP-9), which might be closely related to the process of atherosclerosis (Figure 4B). Consistent with the results in ECs, overexpression of a catalytically inactive mutant, CYLDdel or CYLD$_{C/A}$, showed no change in NF-κB activity, although overexpression of wild-type CYLD significantly decreased NF-κB activity (Figure 4C). These results suggest that CYLD in VSMCs has a suppressive effect on NF-κB-driven cytokine expression via its deubiquitinating action to regulate vascular remodeling.

Because it has recently been reported that CYLD has an anti-proliferative effect via deubiquitination of Bcl-3, which may be upstream of cyclin D1 and the E2F pathway,[9] we further examined these effects of CYLD in VSMCs. Indeed, E2F activity was significantly suppressed by overexpressed CYLD assessed by gel shift mobility assay and reporter gene assay (43% inhibition; $P < 0.05$, compared with control), but not by catalytically inactive CYLD (Figure 5A). Furthermore, cell viability assessed by MTS assay was also suppressed by overexpressed CYLD (20% inhibition; $P < 0.05$, compared with control), but not by catalytically inactive CYLD (Figure 5B).

Figure 4. Effect of CYLD on NF-κB activation in vascular aortic smooth muscle cells. **A:** Overexpression of CYLD significantly attenuated NF-κB activation with or without TNF-α stimulation, as assessed by gel mobility shift assay (**top**) and by means of the luciferase gene driven by the NF-κB biding site (**bottom**) in A7r5. **Top:** Overexpressed CYLD suppressed the binding of NF-κB to the DNA consensus sequence in gel mobility shift assay. **Bottom:** Overexpressed CYLD attenuated NF-κB activity. Control indicates overexpressed GFP gene, and CYLD indicates overexpressed human CYLD. TNF-α indicates treatment with human recombinant TNF-α (10 ng/ml) for 12 hours. $^{*}P < 0.05$ versus control. $^{\#}P < 0.05$ versus TNF-α (−). $N = 6$ per group in triplicate. **B:** Quantitative real-time PCR of TNF-α (10 ng/ml)-induced IL-6 and MMP-9 mRNA expression with or without overexpression of CYLD after treatment with TNF-α (10 ng/ml) for 6 hours. Overexpressed CYLD significantly attenuated TNF-α-induced expression of these NF-κB-regulatory genes. Control indicates overexpressed GFP gene, and CYLD indicates overexpressed human CYLD. TNF-α indicates treatment with human recombinant TNF-α (10 ng/ml) for 6 hours. $^{*}P < 0.05$ versus control. $^{\#}P < 0.05$ versus TNF-α (−). $N = 6$ per group in triplicate. **C:** Effect of catalytically inactive CYLD on NF-κB activity as assessed by means of the luciferase gene driven by the NF-κB biding site in A7r5. Overexpression of CYLD significantly attenuated NF-κB activation, whereas overexpression of a catalytically inactive mutant, CYLDdel or CYLD$_{C/A}$, showed no effect. Control indicates overexpressed GFP gene, and CYLD indicates overexpressed human wild-type CYLD. CYLDdel indicates overexpressed deletion mutant of human CYLD. CYLD$_{C/A}$ indicates overexpression of human CYLD mutant with amino acid replacement. $^{*}P < 0.05$ versus control.

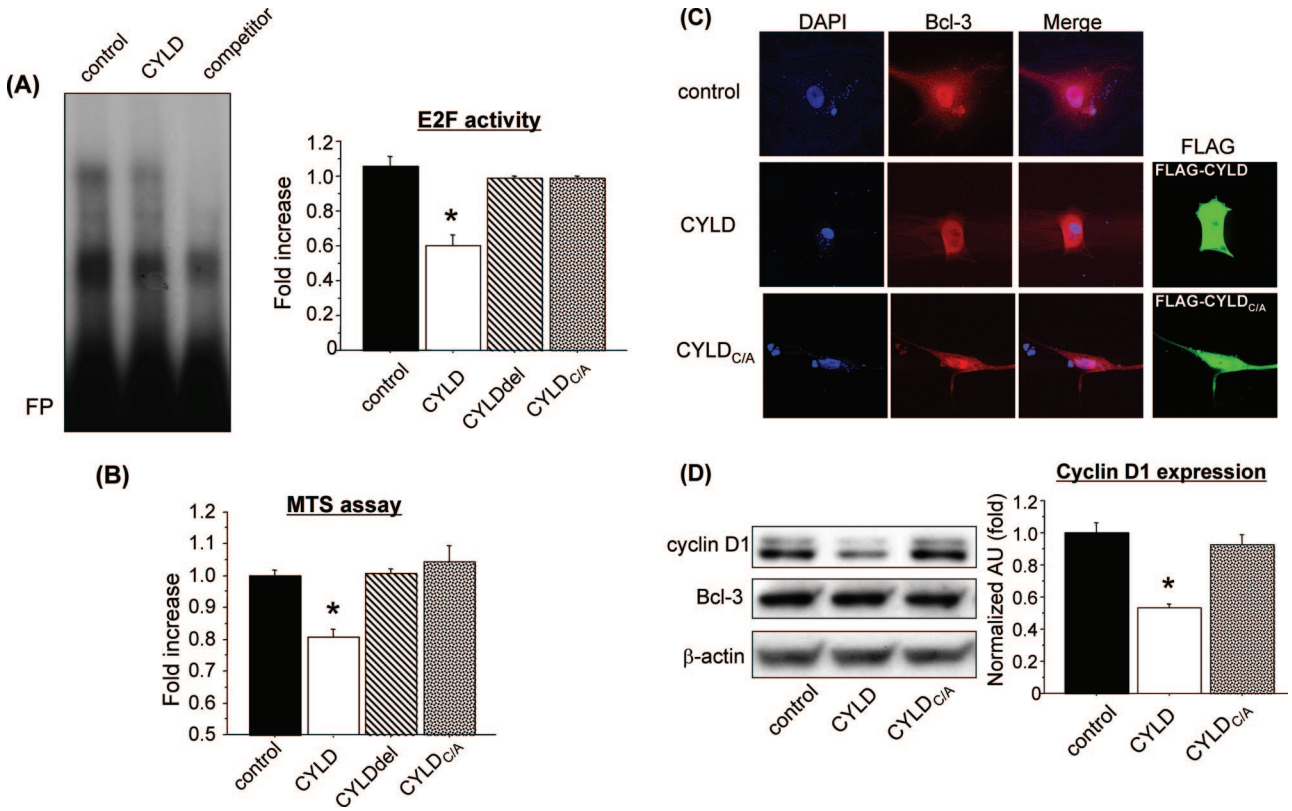

Figure 5. Effect of CYLD on cell proliferation in vascular aortic smooth muscle cells. **A:** Effect of CYLD on E2F activity, as evaluated by means of the luciferase gene driven by the E2F binding site (**right**) and by gel mobility shift assay (**left**) in A7r5. **Left:** Overexpressed CYLD suppressed the binding of E2F to the DNA consensus sequence in gel mobility shift assay. **Right:** Overexpressed wild-type CYLD attenuated E2F activity, whereas overexpressed catalytically inactive CYLD did not. Control indicates overexpressed GFP gene, and CYLD indicates overexpressed human wild-type CYLD. CYLDdel indicates overexpressed deletion mutant of human CYLD. $CYLD_{C/A}$ indicates overexpression of human CYLD mutant with amino acid replacement. $^*P < 0.05$ versus control. $N = 4$ per group in duplicate. **B:** Effect of CYLD on cell viability, as evaluated by MTS assay in A7r5. Overexpressed CYLD suppressed cell viability, whereas overexpression of the catalytically inactive mutant of CYLD, CYLDdel or $CYLD_{C/A}$, did not. Control indicates overexpressed GFP gene, and CYLD indicates overexpressed human wild-type CYLD. CYLDdel indicates overexpression of deletion mutant of human CYLD. $CYLD_{C/A}$ indicates overexpression of human CYLD mutant with amino acid replacement. $^*P < 0.05$ versus control. $N = 4$ per group in duplicate. **C:** Immunostaining analysis of Bcl-3 in HASMCs. **Top:** Immunofluorescent staining in GFP-transfected cells (control); **middle:** FLAG-tagged wild-type CYLD-transfected cells (CYLD); and **bottom:** FLAG-tagged catalytically inactive CYLD (amino acid replacement)-transfected cells ($CYLD_{C/A}$). DAPI indicates nuclear staining (blue), Bcl-3 indicates staining with anti-Bcl-3 antibody (red), and merge indicates staining with both. Overexpressed wild-type CYLD inhibited nuclear translocation of Bcl-3, whereas overexpressed catalytically inactive CYLD did not. **Left:** Immunofluorescent staining with anti-FLAG antibody (green) in CYLD and $CYLD_{C/A}$ to confirm transfection of human CYLD or catalytically inactive CYLD expression in HAECs. **D:** Western blot of cyclin D1 and Bcl-3 in A7r5. Expression of cyclin D1 was down-regulated by overexpressed CYLD, but not overexpressed catalytically inactive CYLD ($CYLD_{C/A}$). The expression level of Bcl-3 was not altered by overexpression of wild-type CYLD or catalytically inactive CYLD. Corresponding β-actin expression was used to standardize loading. Experiments were performed in triplicate. **Right:** Quantification of cyclin D1 expression by densitometry. Cyclin D1 protein levels were corrected using β-actin as an internal control. AU, arbitrary unit. $N = 5$ per group. $^*P < 0.05$ versus control. Original magnifications, ×800 (**C**).

Immunofluorescent staining with anti-Bcl-3 antibody in VSMCs showed that Bcl-3 was located in the nucleus and cytoplasm, whereas in CYLD-transfected VSMCs, Bcl-3 remained in the cytoplasm. Of importance, catalytically inactive CYLD overexpression allowed Bcl-3 to be located predominantly in the nucleus (Figure 5C). Overexpressed CYLD significantly decreased cyclin D1 expression without a significant change in Bcl-3 protein expression, whereas catalytically inactive CYLD did not show a significant change in cyclin D1 expression (Figure 5D). These results suggest that CYLD inhibited SMC proliferation via blockade of the cyclin D1 and E2F pathway, possibly through deubiquitination of Bcl-3.

Functional Analysis of CYLD in in Vivo *Balloon Injury Model of Rat Carotid Artery*

We examined the effect of overexpressed CYLD in a balloon injury model of rat carotid artery by HVJ-liposome method.[13] As shown in Figure 6A, overexpression of CYLD plasmid resulted in significant inhibition of neointimal formation, as quantified by measurement of neointimal and medial area and by calculation of the ratio of neointimal-to-medial area at 2 weeks after balloon injury (ratio of neointimal-to-medial area, 35% inhibition compared with control; $P < 0.01$) (Figure 6A). Accompanied by inhibition of neointimal formation by transfection of CYLD plasmid DNA, inhibition of NF-κB activation was confirmed at 7 days after transfection by immunostaining with anti-p65 (NF-κB subunit) antibody (Figure 6B). The anti-p65 antibody recognizes the epitopes overlapping the nuclear location signal of the subunit of the NF-κB heterodimer, and fairly selectively binds to the activated form of NF-κB. The expression of an NF-κB regulatory protein, ICAM-1, was also suppressed in the neointima of the CYLD-overexpressing group, as assessed by immunostaining at 7 days after transfection (Figure 6C). We further examined the proliferation of vascular cells in

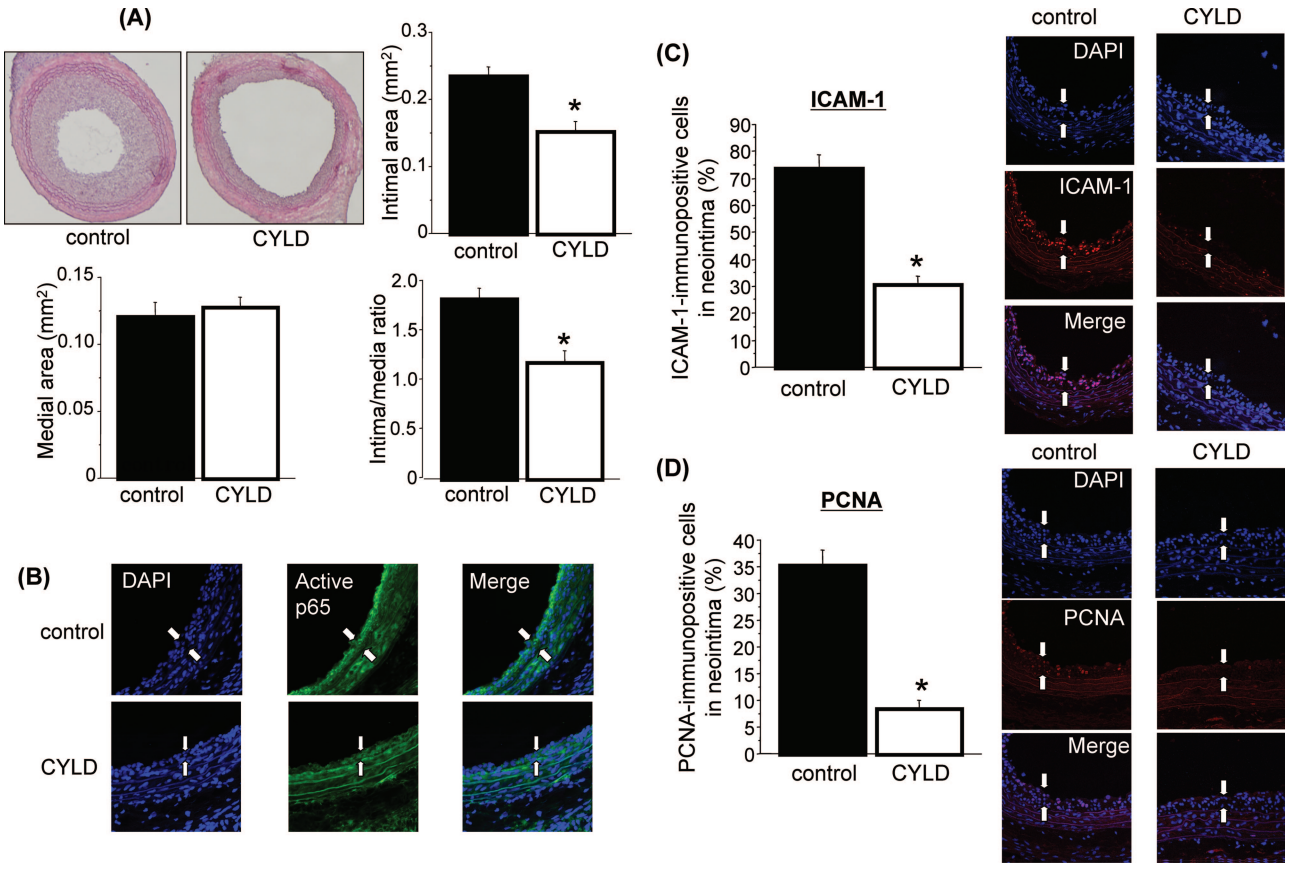

Figure 6. Effects of CYLD on balloon-injured arteries. **A:** Effect of overexpressed CYLD on neointimal formation in rat balloon injury model at 14 days after transfection. **Top left:** Representative cross sections of balloon-injured vessels with H&E staining. Control indicates transfection of LacZ plasmid. CYLD indicates transfection of CYLD plasmid. **Top right**, **bottom left**, and **bottom right:** Quantification of intimal area, medial area, and ratio of neointimal-to-medial area in the rat balloon injury model at 14 days after transfection, respectively. $^*P < 0.01$ versus control. NS indicates not significant. Control group contains seven animals; CYLD group contains seven animals. **B:** Effect of overexpressed CYLD on NF-κB inactivation in rat balloon injury model at 7 days after transfection, as assessed by immunostaining with anti-p65 antibody (green;). Control indicates transfection of LacZ plasmid. CYLD indicates transfection of CYLD plasmid. DAPI indicates nuclear staining (blue). Merge indicates staining with both. The area between the **white arrows** indicates neointimal formation. **C** and **D:** Representative photomicrographs of immunostaining with anti-ICAM-1 and anti-PCNA antibody and their quantification to evaluate the effect of overexpressed CYLD on NF-κB inactivation and cell proliferation in a rat balloon injury model at 7 days after transfection. **C**, **Right:** Representative cross section stained with anti-ICAM-1 antibody (red); **left:** quantification of ICAM-1-immunopositive cells in neointima. **D**, **Right:** Representative cross section stained with anti-PCNA antibody (red); **left:** quantification of PCNA-immunopositive cells in neointima. Control indicates transfection of LacZ plasmid. CYLD indicates transfection of CYLD plasmid. DAPI indicates nuclear staining (blue). Merge indicates staining with DAPI and anti-ICAM-1 antibody (**C**) or DAPI and anti-PCNA antibody (**D**). The area between the **white arrows** indicates neointimal formation. Control group contains four animals; CYLD group contains four animals. Original magnifications: ×40 (**A**); ×500 (**B**); ×200 (**C**, **D**).

injured arteries. PCNA-stained nuclei were increased in the injured vessels at 7 days after balloon injury, whereas few PCNA-stained nuclei were found in vessels transfected with CYLD (Figure 6D). These results suggest that CYLD may attenuate vascular remodeling after balloon injury through anti-inflammatory and anti-proliferative actions.

Discussion

Ubiquitination plays a crucial role in various cellular processes, including signal transduction, cell differentiation, and stress responses.[4] On the other hand, a deubiquitination system also exists in cells, and DUBs remove polyubiquitin chains from and alter the date of specific target proteins. The present study revealed that the DUB, CYLD, was expressed in vascular cells and in atherosclerotic lesions. Because CYLD modulates the NF-κB pathway, a crucial mediator of inflammation,[15–18] these data suggest that CYLD may regulate vascular remodeling.

Previous studies have suggested that the DUB activity of CYLD is pivotal in modulating tumor necrosis factor receptor (TNFR)-induced NF-κB activation.[17,19,20] TNFR engagement recruits the adaptor molecule TNFR-associated factor 2 (TRAF2), which autoubiquitinates and activates itself. TRAF2 activation ultimately leads to phosphorylation and degradation of the inhibitor, IκB-α, followed by the release and nuclear translocation of NF-κB. The inhibition of NF-κB activation by CYLD is mediated, at least in part, by the deubiquitination and inactivation of TRAF2 and, to a lesser extent, TRAF6.[19,20] In this study, we hypothesized that CYLD played an important role as an endogenous suppressor to regulate inflammation or vascular remodeling. Although the phenotype of CYLD-deficient mice was not so severe, activation of B cells, T cells, and myeloid cells by mediators of

innate and adaptive immunity resulted in enhanced NF-κB and JNK activity associated with increased TRAF2.[18] In addition, CYLD-deficient mice were more susceptible to colonic inflammation[18] and skin tumors[9] because of markedly elevated tumor cell proliferation. In this study, we also confirmed that CYLD deubiquitinated TRAF2, leading to inactivation of the NF-κB pathway in ECs, although CYLD may have other targets to suppress NF-κB activity. A recent report showed several steps of a signaling pathway in which CYLD undertakes the principal task of controlling the nuclear translocation of Bcl-3,[9] which in turn alters the transcriptional properties of the NF-κB p50 and p52 homodimers, leading to cellular proliferation through activation of the cyclin D1 gene.[21–23] After the translocation of Bcl-3 from the cytoplasm to the perinuclear region, CYLD removes K63-linked polyubiquitin chains from Bcl-3, which prevents Bcl-3 from translocating into the nucleus.[9] In this study, we also assessed the association of Bcl-3 and CYLD in VSMCs. Interestingly, in VSMCs, Bcl-3 was endogenously expressed in both the nucleus and cytoplasm, whereas CYLD prevented Bcl-3 translocation into the nucleus, possibly via its deubiquitinating action. Of importance, overexpressed CYLD reduced cyclin D1 expression and E2F activity, similar to the findings of a previous report in epithelial cancer cells.[9] These data suggest that CYLD controls inflammation through TRAF signaling and NF-κB p65/p50 activation or cellular proliferation through Bcl-3 activation and NF-κB p50/p52 binding.

Recent findings revealed an autoregulatory feedback loop in which TNF-α-induced NF-κB activation induced CYLD, which in turn led to inhibition of NF-κB signaling.[24,25] NF-κB-dependent transcriptional induction of its own inhibitor IκB-α has been identified as an important mechanism to ensure the transient nature of NF-κB induction.[26] In contrast to the negative feedback mechanism in relation to IκB-α, the NF-κB-dependent induction of CYLD may play a more important role in controlling the delayed action of NF-κB induction. Thus, the NF-κB-dependent induction of both IκBα and CYLD may be essential for ensuring tight control of NF-κB activation in the transient and the delayed or persistent phase.[26–28] In this study, we also confirmed up-regulation of CYLD expression by treatment with TNF-α in vascular cells, and delayed induction of CYLD in the neointima of balloon-injured arteries which, in turn, may be a negative regulator of NF-κB activation. We speculate that this negative regulator in the late phase or persistent phase might be important in chronic disease processes, such as atherosclerosis.

Recently, Marfella and colleagues[29,30] have demonstrated that the ubiquitin-proteasome activity in human plaques was associated with inflammation-induced plaque rupture, possibly through up-regulation of NF-κB-mediated inflammatory pathways. It has also been reported that antioxidant vitamin supplementation prevents NF-κB activation and the accumulation of ubiquitin conjugates.[31] Furthermore, in an autopsy-based immunohistochemical study, ubiquitin/ubiquitin conjugates were increased and co-localized with macrophages and terminal dUTP nick-end labeling-positive cells in the lipid core.[32] These data suggest that the critical link between ubiquitination and inflammation is the transcription factor, NF-κB. Initial reports indicate that proteasome inhibition might be an effective therapeutic strategy for the prevention of atherosclerosis and restenosis.[4,33] Indeed, aspirin and statins, two of the most successful drugs in the prevention of cardiovascular events, both possess inhibitory effects on proteasome activity.[34,35] Thus, DUB may be a novel therapeutic target to attenuate the activity of ubiquitination. Indeed, *in vivo* gene transfer of CYLD to balloon-injured artery efficiently attenuated neointimal formation, accompanied by NF-κB inactivation. Although CYLD-deficient mice do not display any apparent abnormalities in vascular development,[18] we speculate that the deubiquitinating effect of CYLD might be redundant in vascular development. Further study would be of benefit.

In summary, the present study demonstrated that a DUB, CYLD, was expressed in vascular ECs and VSMCs and that CYLD may participate in vascular remodeling via inhibition of NF-κB or E2F activity. These data suggest that CYLD may be a potential therapeutic target for the modulation or prevention of vascular remodeling and atherosclerosis.

References

1. Haglund K, Dikic I: Ubiquitylation and cell signaling. EMBO J 2005, 24:3353–3359
2. Gibbons GH, Dzau VJ: Molecular therapies for vascular diseases. Science 1996, 272:689–693
3. D'Andrea A, Pellman D: Deubiquitinating enzymes: a new class of biological regulators. Crit Rev Biochem Mol Biol 1998, 33:337–352
4. Meiners S, Laule M, Rother W, Guenther C, Prauka I, Muschick P, Baumann G, Kloetzel PM, Stangl K: Ubiquitin-proteasome pathway as a new target for the prevention of restenosis. Circulation 2002, 105:483–489
5. Bignell GR, Warren W, Seal S, Takahashi M, Rapley E, Barfoot R, Green H, Brown C, Biggs PJ, Lakhani SR, Jones C, Hansen J, Blair E, Hofmann B, Siebert R, Turner G, Evans DG, Schrander-Stumpel C, Beemer FA, van Den Ouweland A, Halley D, Delpech B, Cleveland MG, Leigh I, Leisti J, Rasmussen S: Identification of the familial cylindromatosis tumour-suppressor gene. Nat Genet 2000, 25: 160–165
6. Yoshimura S, Morishita R, Hayashi K, Yamamoto K, Nakagami H, Kaneda Y, Sakai N, Ogihara T: Inhibition of intimal hyperplasia after balloon injury in rat carotid artery model using cis-element 'decoy' of nuclear factor-kappaB binding site as a novel molecular strategy. Gene Ther 2001, 8:1635–1642
7. Nakagami H, Morishita R, Yamamoto K, Taniyama Y, Aoki M, Matsumoto K, Nakamura T, Kaneda Y, Horiuchi M, Ogihara T: Mitogenic and anti-apoptotic actions of hepatocyte growth factor through ERK. STAT3, and AKT in endothelial cells. Hypertension 2001, 37:581–586
8. Matsushita H, Morishita R, Nata T, Aoki M, Nakagami H, Taniyama Y, Yamamoto K, Higaki J, Yasufumi K, Ogihara T: Hypoxia-induced endothelial apoptosis through nuclear factor-kappaB (NF-kappaB)-mediated bcl-2 suppression: in vivo evidence of the importance of NF-kappaB in endothelial cell regulation. Circ Res 2000, 86:974–981
9. Massoumi R, Chmielarska K, Hennecke K, Pfeifer A, Fassler R: Cyld inhibits tumor cell proliferation by blocking Bcl-3-dependent NF-kappaB signaling. Cell 2006, 125:665–677
10. Niwa H, Yamamura K, Miyazaki J: Efficient selection for high-expression transfectants with a novel eukaryotic vector. Gene 1991, 108:193–199
11. Nakagami H, Takemoto M, Liao JK: NADPH oxidase-derived superoxide anion mediates angiotensin II-induced cardiac hypertrophy. J Mol Cell Cardiol 2003, 35:851–859
12. Morishita R, Gibbons GH, Ellison KE, Nakajima M, Zhang L, Kaneda Y, Ogihara T, Dzau VJ: Single intraluminal delivery of antisense cdc2

kinase and proliferating-cell nuclear antigen oligonucleotides results in chronic inhibition of neointimal hyperplasia. Proc Natl Acad Sci USA 1993, 90:8474–8478
13. Yin X, Yutani C, Ikeda Y, Enjyoji K, Ishibashi-Ueda H, Yasuda S, Tsukamoto Y, Nonogi H, Kaneda Y, Kato H: Tissue factor pathway inhibitor gene delivery using HVJ-AVE liposomes markedly reduces restenosis in atherosclerotic arteries. Cardiovasc Res 2002, 56: 454–463
14. Ouchi N, Kihara S, Arita Y, Maeda K, Kuriyama H, Okamoto Y, Hotta K, Nishida M, Takahashi M, Nakamura T, Yamashita S, Funahashi T, Matsuzawa Y: Novel modulator for endothelial adhesion molecules: adipocyte-derived plasma protein adiponectin. Circulation 1999, 100:2473–2476
15. Chen ZJ: Ubiquitin signalling in the NF-kappaB pathway. Nat Cell Biol 2005, 7:758–765
16. Deng L, Wang C, Spencer E, Yang L, Braun A, You J, Slaughter C, Pickart C, Chen ZJ: Activation of the IkappaB kinase complex by TRAF6 requires a dimeric ubiquitin-conjugating enzyme complex and a unique polyubiquitin chain. Cell 2000, 103:351–361
17. Kovalenko A, Chable-Bessia C, Cantarella G, Israel A, Wallach D, Courtois G: The tumour suppressor CYLD negatively regulates NF-kappaB signalling by deubiquitination. Nature 2003, 424:801–805
18. Zhang J, Stirling B, Temmerman ST, Ma CA, Fuss IJ, Derry JM, Jain A: Impaired regulation of NF-kappaB and increased susceptibility to colitis-associated tumorigenesis in CYLD-deficient mice. J Clin Invest 2006, 116:3042–3049
19. Brummelkamp TR, Nijman SM, Dirac AM, Bernards R: Loss of the cylindromatosis tumour suppressor inhibits apoptosis by activating NF-kappaB. Nature 2003, 424:797–801
20. Trompouki E, Hatzivassiliou E, Tsichritzis T, Farmer H, Ashworth A, Mosialos G: CYLD is a deubiquitinating enzyme that negatively regulates NF-kappaB activation by TNFR family members. Nature 2003, 424:793–796
21. Thornburg NJ, Pathmanathan R, Raab-Traub N: Activation of nuclear factor-kappaB p50 homodimer/Bcl-3 complexes in nasopharyngeal carcinoma. Cancer Res 2003, 63:8293–8301
22. Cogswell PC, Guttridge DC, Funkhouser WK, Baldwin AS Jr: Selective activation of NF-kappa B subunits in human breast cancer: potential roles for NF-kappa B2/p52 and for Bcl-3. Oncogene 2000, 19:1123–1131
23. Budunova IV, Perez P, Vaden VR, Spiegelman VS, Slaga TJ, Jorcano JL: Increased expression of p50-NF-kappaB and constitutive activation of NF-kappaB transcription factors during mouse skin carcinogenesis. Oncogene 1999, 18:7423–7431
24. Jono H, Lim JH, Chen LF, Xu H, Trompouki E, Pan ZK, Mosialos G, Li JD: NF-kappaB is essential for induction of CYLD, the negative regulator of NF-kappaB: evidence for a novel inducible autoregulatory feedback pathway. J Biol Chem 2004, 279:36171–36174
25. Reiley W, Zhang M, Wu X, Granger E, Sun SC: Regulation of the deubiquitinating enzyme CYLD by IkappaB kinase gamma-dependent phosphorylation. Mol Cell Biol 2005, 25:3886–3895
26. Schmidt C, Peng B, Li Z, Sclabas GM, Fujioka S, Niu J, Schmidt-Supprian M, Evans DB, Abbruzzese JL, Chiao PJ: Mechanisms of proinflammatory cytokine-induced biphasic NF-kappaB activation. Mol Cell 2003, 12:1287–1300
27. Chen ZJ, Parent L, Maniatis T: Site-specific phosphorylation of IkappaBalpha by a novel ubiquitination-dependent protein kinase activity. Cell 1996, 84:853–862
28. Chen L, Fischle W, Verdin E, Greene WC: Duration of nuclear NF-kappaB action regulated by reversible acetylation. Science 2001, 293:1653–1657
29. Marfella R, D'Amico M, Di Filippo C, Baldi A, Siniscalchi M, Sasso FC, Portoghese M, Carbonara O, Crescenzi B, Sangiuolo P, Nicoletti GF, Rossiello R, Ferraraccio F, Cacciapuoti F, Verza M, Coppola L, Rossi F, Paolisso G: Increased activity of the ubiquitin-proteasome system in patients with symptomatic carotid disease is associated with enhanced inflammation and may destabilize the atherosclerotic plaque: effects of rosiglitazone treatment. J Am Coll Cardiol 2006, 47: 2444–2455
30. Marfella R, D'Amico M, Esposito K, Baldi A, Di Filippo C, Siniscalchi M, Sasso FC, Portoghese M, Cirillo F, Cacciapuoti F, Carbonara O, Crescenzi B, Baldi F, Ceriello A, Nicoletti GF, D'Andrea F, Verza M, Coppola L, Rossi F, Giugliano D: The ubiquitin-proteasome system and inflammatory activity in diabetic atherosclerotic plaques: effects of rosiglitazone treatment. Diabetes 2006, 55:622–632
31. Rodriguez-Porcel M, Lerman LO, Holmes DR Jr, Richardson D, Napoli C, Lerman A: Chronic antioxidant supplementation attenuates nuclear factor-kappa B activation and preserves endothelial function in hypercholesterolemic pigs. Cardiovasc Res 2002, 53:1010–1018
32. Herrmann J, Edwards WD, Holmes DR Jr, Shogren KL, Lerman LO, Ciechanover A, Lerman A: Increased ubiquitin immunoreactivity in unstable atherosclerotic plaques associated with acute coronary syndromes. J Am Coll Cardiol 2002, 40:1919–1927
33. Thyberg J, Blomgren K: Effects of proteasome and calpain inhibitors on the structural reorganization and proliferation of vascular smooth muscle cells in primary culture. Lab Invest 1999, 79:1077–1088
34. Dikshit P, Chatterjee M, Goswami A, Mishra A, Jana NR: Aspirin induces apoptosis through the inhibition of proteasome function. J Biol Chem 2006, 281:29228–29235
35. Wójcik C, Bury M, Stoklosa T, Giermasz A, Feleszko W, Mlynarczuk I, Pleban E, Basak G, Omura S, Jakobisiak M: Lovastatin and simvastatin are modulators of the proteasome. Int J Biochem Cell Biol 2000, 32:957–965